SUPPORTING INFORMATION

Advanced Architectural Amorphous Co@PAT Electrocatalyst: Flexible and Sustainable Tri-functional Water Oxidation and STH Conversion for Energy Future

Murugan Vijayarangan, Muthukumaran Sangamithirai, Venkatachalam Ashok, Jayaraman Jayabharathi and Venugopal Thanikachalam*

Department of Chemistry, Material Science Lab, Annamalai University, Annamalai Nagar, Tamil Nadu-608 002, India.

SI-I. Materials and Characterization

1.1 Materials

Cobalt nitrate was purchased from Sisco CHEM PLTD; ferric chloride from; aminothiazole from Sigma Aldrich and double distilled (DI) water. Nickel foam was purchased from Vritra technologies Delhi India. All the reagents were analytical grade and used without further purification.

1.2 Physical characterization

The morphology of 4R Co@PAT was determined by using field emission scanning electron microscope (FE-SEM) CARL ZEISS –SIGMA 300 with energy dispersive X-ray spectra (EDX) operated at 30 kV. JEOL, JEM-2100 Plus was used to record transmission electron microscope (TEM) image of the nanomaterials and selected area electron diffraction (SAED) pattern was taken from JEOL, JEM-2100 Plus. X-ray diffraction (XRD) of Co@PAT was recorded with BRUKER D8 ADVANCE ECO-POWDER X-RAY DIFFRACTION (XRD). Fourier transform infrared (FT-IR) spectra of CNS and Co@PAT were recorded on Shimadzu IRTracer-100. The elemental composition of Co@PAT were analyzed by XPS (Xray photoelectron spectroscopy) with K-Alpha-KAN9954133 SURFACE ANALYSIS spectrometer. Inductively coupled plasma-optical emission spectroscopy (ICP-OES) used to record with Avio 560 Max. UV–vis diffuse reflectance spectroscopy (UV-DRS) was used to record with Multiskan SkyHigh Microplate readers, make: varian model: 5000. BELSORP-maxII (BELSORP – series) from Microtrac BEL Corp Brunauer-Emmett-Teller (BET) surface area analyser.

1.3 Preparation of electrode and electrochemical characterization

A standard three-electrode system connected to biologic electrochemical workstation SP-200 potentiostat at room temperature was used to determine the electrochemical measurements for samples. The Co@PAT on glassy carbon electrode (GCE) and on Nickel foam (NF) with 3 mm in diameter were used as the working electrodes. Pt as the counter

electrode, Ag/AgCl (3M KCl) as the reference electrode. The working NF electrode was washed with 1.0 M HCl to remove oxide layer on the nickel surface, then washed with water, acetone and dried. In this work, the electrocatalyst ink was prepared by mixing 4.0 mg of catalyst in 1.0 ml solvent mixture of Nafion (5 wt %) and water in v/v ratio of 1/9 for 20 min. in an ultrasonicator. Commercially available catalyst (IrO_2) and bare NF was used. About 1.0 mg/ml of commercial IrO_2 suspension was prepared by following the similar methodology for comparison and bare NF was used directly. The slurry was drop casting on a precleaned NF electrode and the electrode was allowed to dry at 70 °C before measurement (catalyst loading 0.5 mg cm^{-2}). The freshly synthesized catalyst and commercial IrO_2 catalyst have been used directly as working electrode without further treatment. All measurements were carried out in 1.0 M KOH. The working NF electrode was washed with 1.0 M HCl to remove oxide layer on the nickel surface, then washed with water, acetone and dried.

As for the electrochemical measurements, the reference electrode was calibrated with respect to a reversible hydrogen electrode (RHE). Linear sweep voltammetry (LSV) was conducted in 1.0 M KOH solution with a scanning at 10 mV s-1 and LSV curves in OER were performed in a potential window of 1.0 to 1.8 V vs. RHE. The respect to the Tafel slope was calculated from the corresponding polarisation curve. The stability was recorded in chronopotentiometry and chronoamperometry. The electrochemical double layer capacitance (C_{dl}) was determined by the CV in the non-faradaic region from1.11 to 1.31 V vs. RHE with different scan rates. The corresponding electrochemical surface area (ECSA) was calculated by the C_{dl} based on the following equation: ECSA = C_{dl} /Cs, in which the Cs is the specific capacitance of the electrocatalyst. Moreover, the electrochemical impedance spectroscopy (EIS) measurements were performed in a frequency range from 100 kHz to 10 mHz with sinusoidal perturbation amplitude of 0.5 V, in which the semicircle of the Nyquist plot can efficiently reflect the electrocatalytic kinetics. The turnover frequency (TOF) rate of evolved

molecular O_2 per surface active site per second can be calculated. The overpotential used for the calculation of TOF was set at potential of 1. 60 V vs RHE. The overall water splitting measurement was performed in a two-electrode system with the electrocatalyst ink coated on NF surface as anode and Pt/C as cathode.

SI-II. Figures

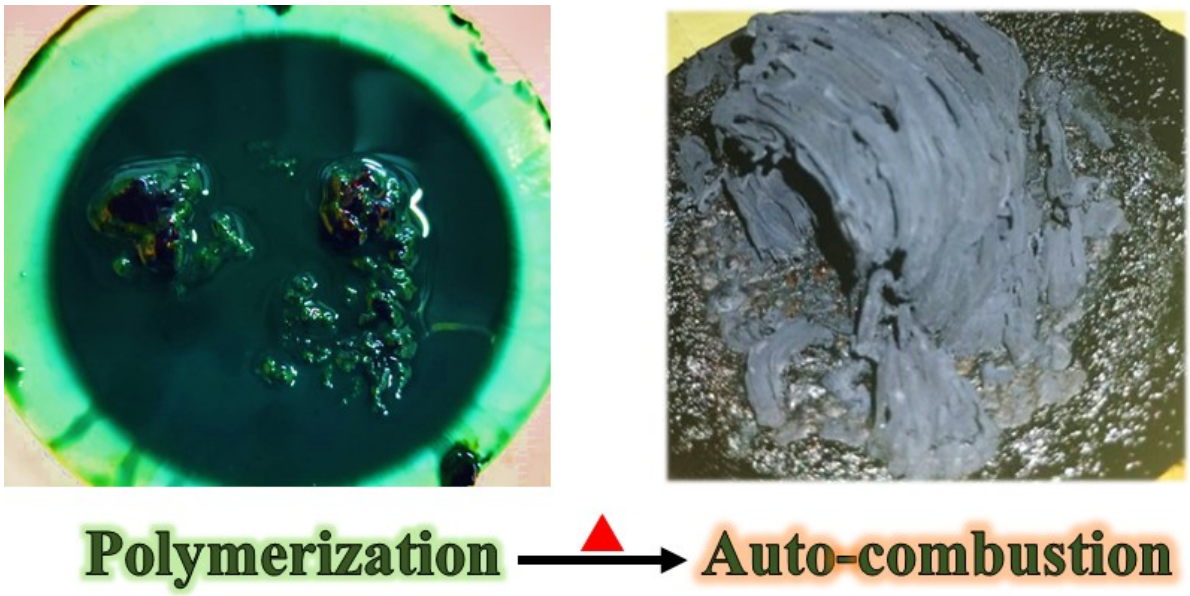

Figure S1. Combustion process of Co@PAT

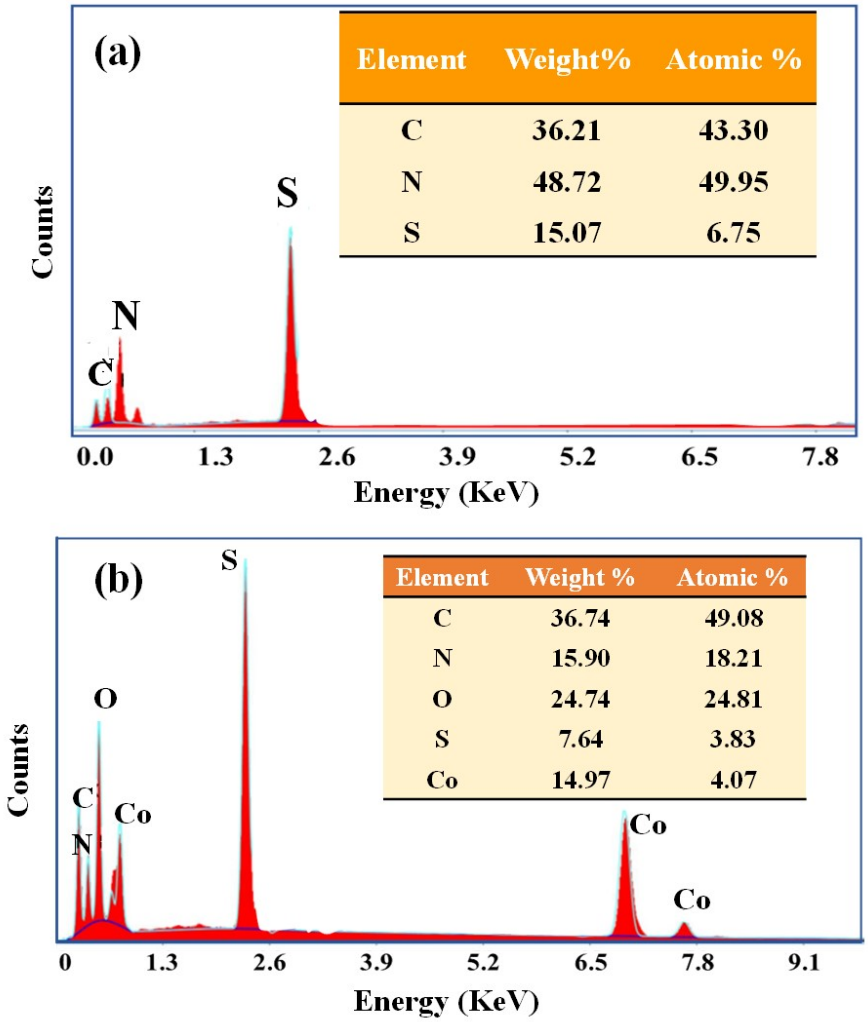

Figure S2. EDX spectra of (a) CNS and (b) 4R Co@PAT with elemental composition.

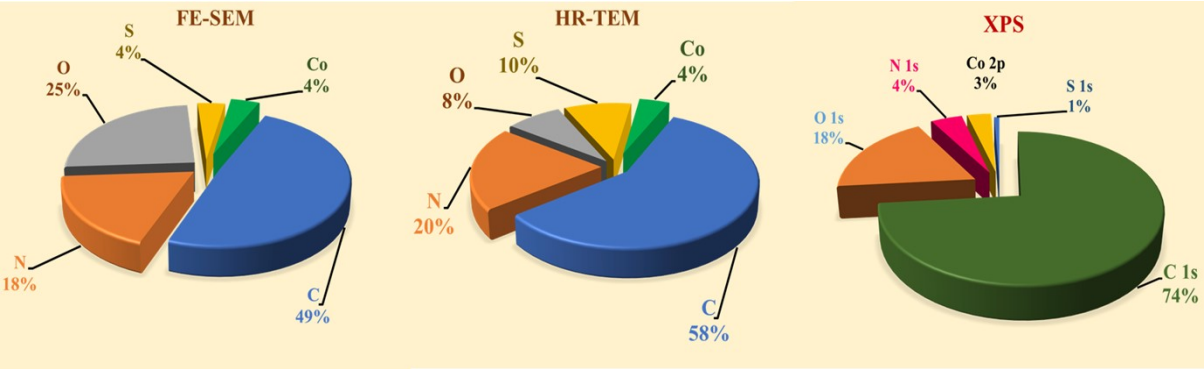

Figure S3. Atomic % from physicochemical analysis.

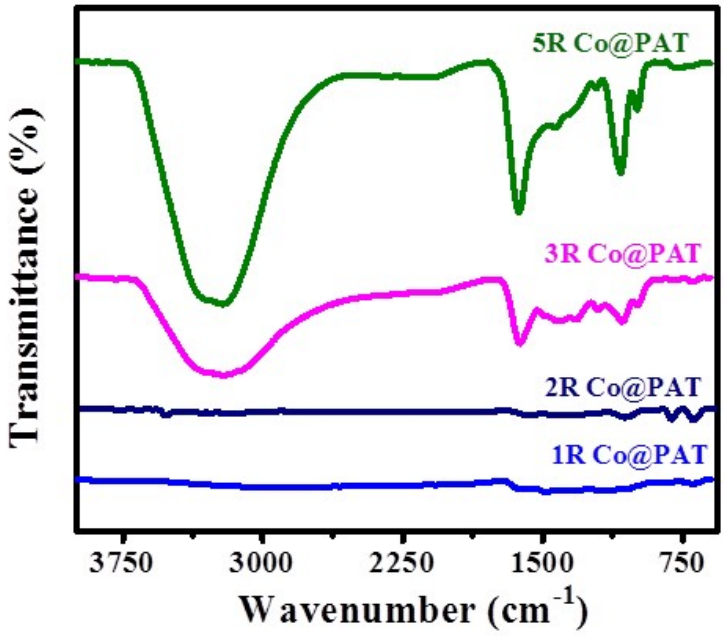

Figure S4. FT-IR spectra of 1R Co@PAT, 2R Co@PAT, 3R Co@PAT and 5R Co@PAT

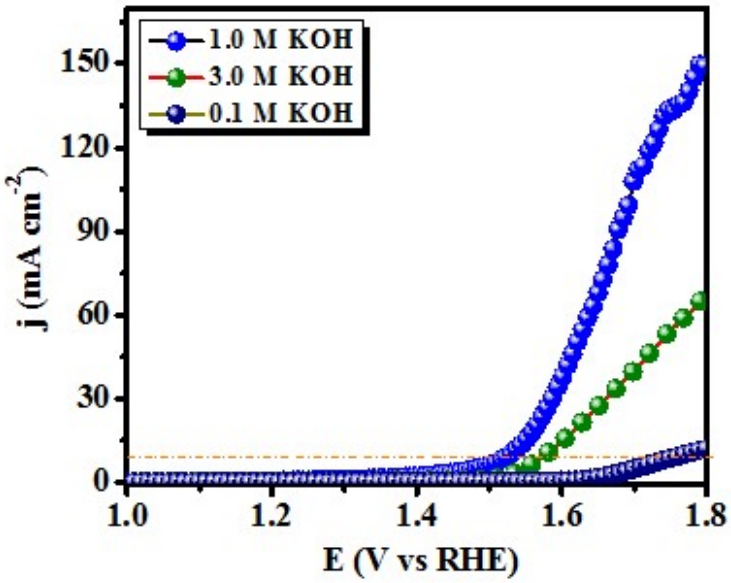

Figure S5. Alkaline comparison of 4R Co@PAT in GC electrode

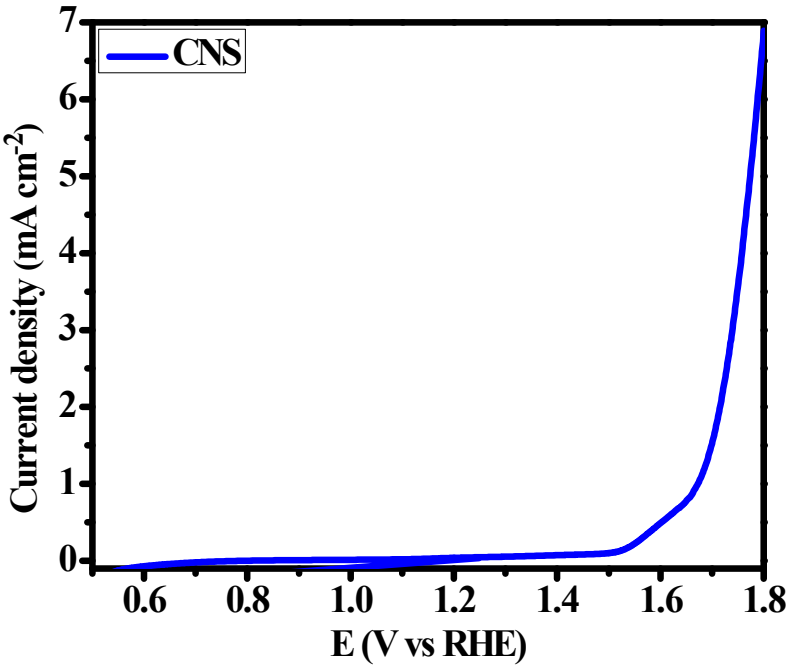

Figure S6. Polarisation curve of CNS in glassy carbon electrode.

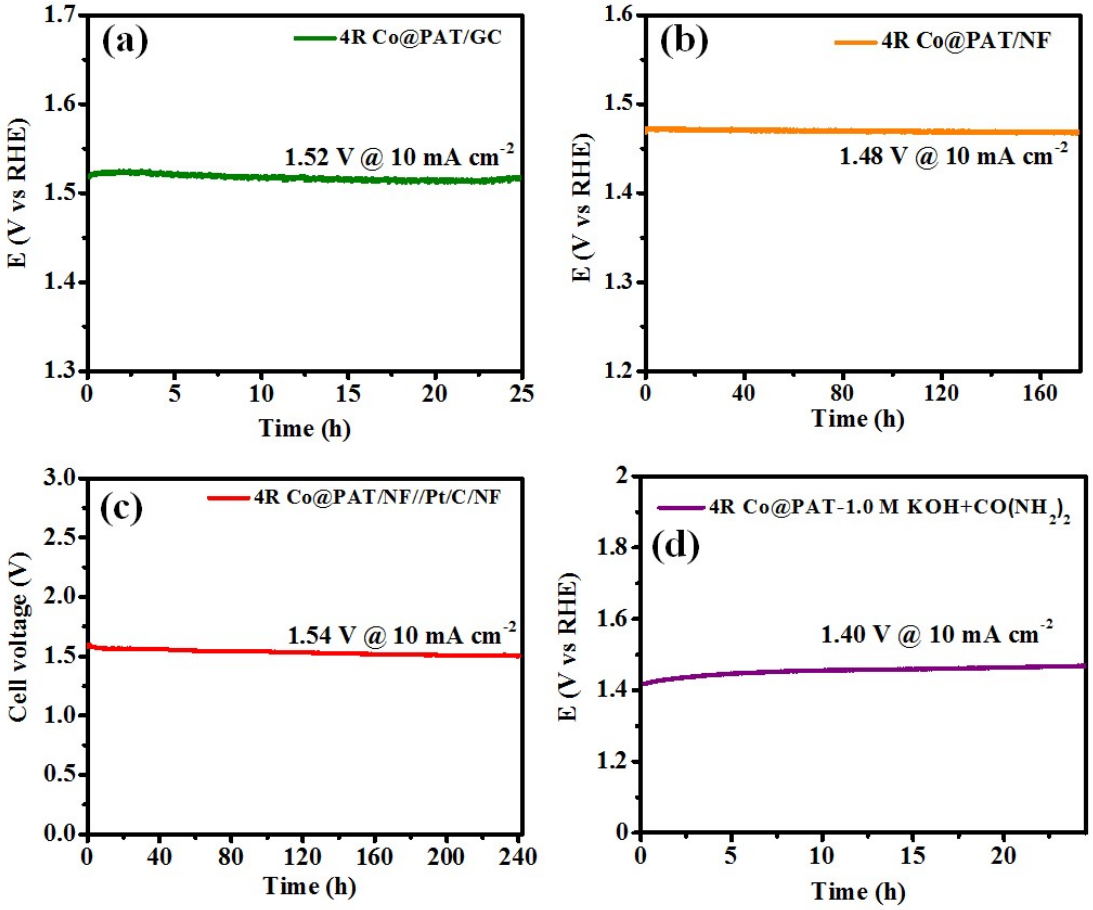

Figure S7. Choronopotentiometry durability of (a) 4R Co@PAT/GC, (b) 4R Co@PAT/NF, (c) 4R Co@PAT/NF//Pt/C/NF and (d) 4R Co@PAT - 1.0 M KOH+$CO(NH_2)_2$.

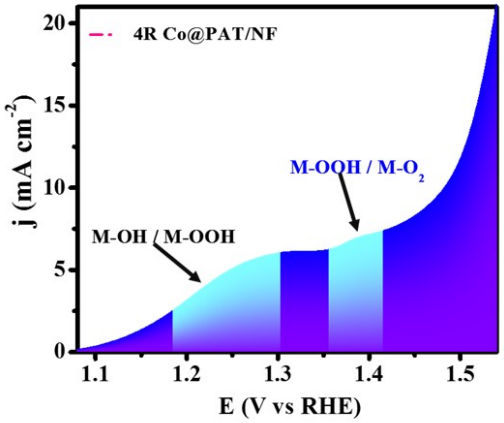

$$AS + OH^- \rightarrow AS\text{-}OH^* + e^-;$$

$$AS\text{-}OH^* + OH^- \rightarrow AS\text{-}O^* + H_2O + e^-;$$

$$AS\text{-}O^* + OH^- \rightarrow AS\text{-}OOH^* + e^-;$$

$$AS\text{-}OOH^* + OH^- \rightarrow AS\text{-}OO^- + H_2O$$

$$AS\text{-}OO^- \rightarrow AS + O_2 + e^-$$

(AS* denotes the active site on the surface of the catalyst)

Figure S8. Intermediate formation of oxygen evolution.

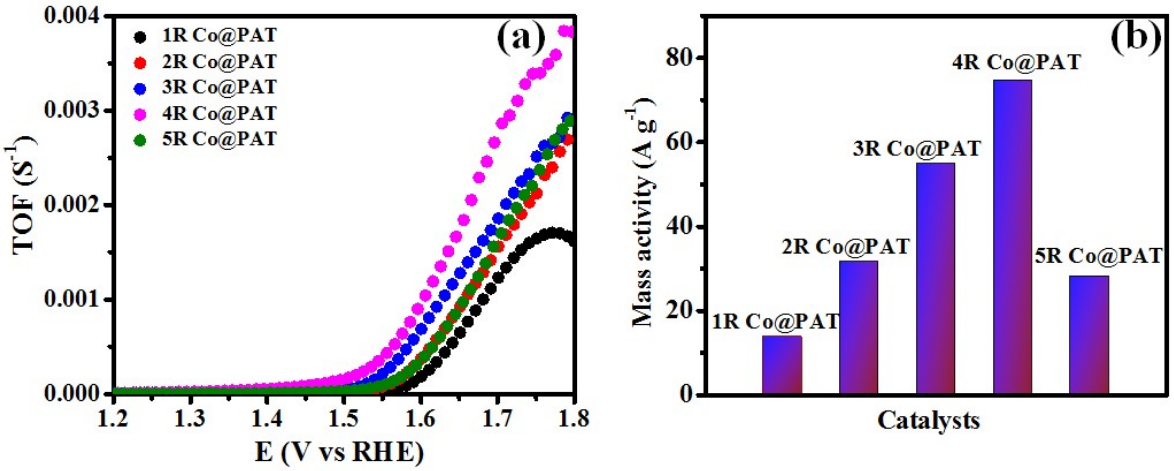

Figure S9. (a) TOF normalized and (b) mass activity of Co@PAT.

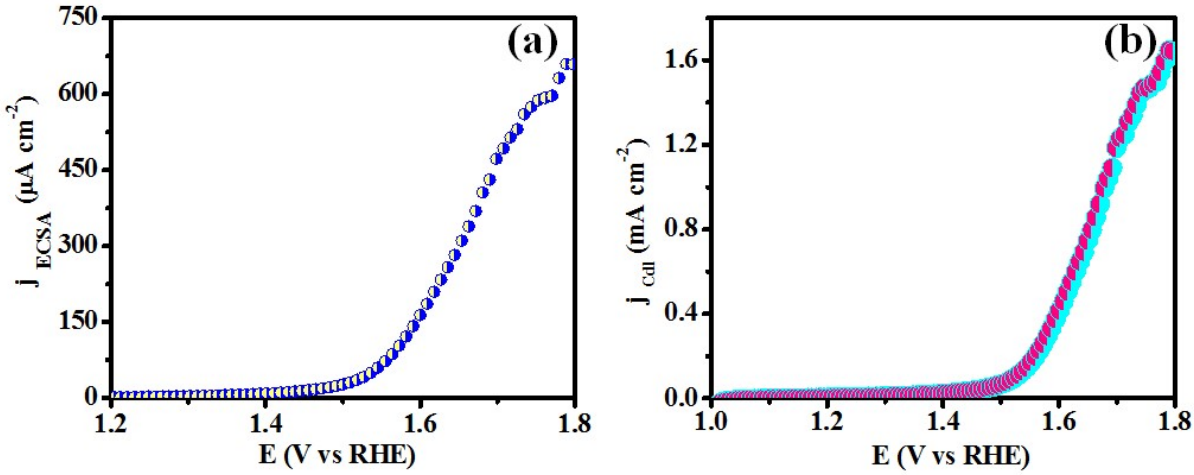

Figure S10. (a and b) ECSA and C_{dl} normalized curve of 4R Co@PAT.

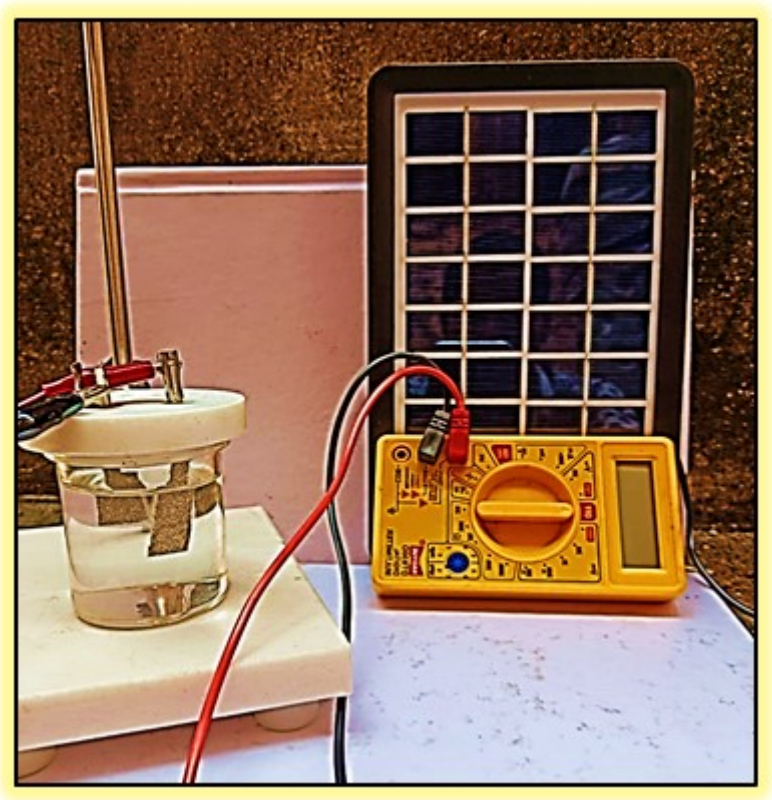

Figure S11. General solar cell setup

SI-III. Calculation

Overpotential (η) of OER was calculated with the equation:

$$\eta_{OER} = 1.23 - E_{RHE}$$

Double layer capacitance (C_{dl}) was determined by measuring cyclic voltammograms (CVs) with multiple scan rates in non-faradaic potential region for OER with various scan rates from 20 to 140 mV s^{-1}. Electrochemically active surface areas (ECSAs) were calculated by dividing the C_{dl} with specific capacitance (C_s) of the sample according to equation:

$$ECSA = C_{dl} / C_s$$

$$\text{ECSA-normalized current density} = \text{current density (j)} \times C_s / C_{dl}$$

Where Cs is specific capacitances of per unit area for sample identical electrolyte conditions. For our estimates of surface area, Cs is chosen as 0.04 mF·cm^{-2} in 1.0 M KOH

Roughness factor can be calculated by the following equation:

$$RF = ECSA / GSA$$

GSA is chosen as 0.0706 for GC electrode

Turnover frequency and Mass activity.

$$\text{Turnover frequency (TOF)} = (J \times A) / (4 \times F \times n)$$

$$\text{Mass activity} = J / m$$

Where J (A cm^{-2}) is the current density at a specific overpotential, A (0.07065 cm^2) is the area of the GCE, F (96485.3321 mol C^{-1}) is the Faraday constant, n is the total moles number of the active metal sites (Co) on the catalyst that are deposited onto the electrode (assuming all metal are active during OER, the TOF value is the lower bound), and m is the mass loading of the catalyst (0.0005 g cm^{-2}).

Faradaic efficiency.

In the water electrolysis process, to quantify the O_2 and H_2 gases produced, the gas chromatography technique is used to measure the faradic efficiency. A 250 ml five-neck sealed

glass cell was used to measure the amount of O_2 and H_2. The glass cell has purged with Ar (99.9%) for 2 hours before starting the experiment. The electrolysis was performed with Co@CN-NPs as a working electrode whereas platinum electrode and Ag/AgCl in 3.0 M KCl was used as counter and reference electrode. The catalyst loading on the electrode surface was 0.12 $mg.cm^{-2}$. The chronopotentiometry experiment was performed with Co@CN-NPs modified working electrode at current density of 10 $mAcm^{-2}$ and at 20-min time interval gas was analyzed with GC instrument (Thermo scientific, Model: Trace 1110) with thermal conductive detector (TCD) and argon as carrier gas.

The Faradic efficiency (%)

$$= \frac{(\text{number of moles of gas produced experimentally for a certain time}) * 100}{\text{Theoretically calculated gas production (in mole) for the same time}}$$

The theoretical amount of gas (O_2 and H_2) was calculated from accumulated charge during potentiostatic electrolysis by assuming 100% faradic efficiency.

Theoretical amount (n in mole) of gas (H_2, O_2) = Q / (n * F) = (I * t) / (n * F)

Where I is the current in Amp, t is time in sec, n is the number of electrons which is 2 for HER and 4 for OER and F is the Faraday constant (96485.3 $C.mol^{-1}$).

SI-IV. Tables

Table S1. OER alkaline comparison of 4R Co@PAT catalyst

Catalyst	η_{10} - OER (mV)		
	0.1 M KOH	1.0 M KOH	3.0 M KOH
4R Co@PAT	490	250	340

Table S2. Important parameters of the present work.

Catalyst	GC		NF		R_{ct} (Ω)	C_{dl} (mF cm^{-2})	RF	TOF (S^{-1})
	η_{10} (mV)	Tafel (mV dec^{-1})	η_{10} (mV)	Tafel (mV dec^{-1})				
1R Co@PAT	381	109	312	51	2.85	31.6	1118.9	0.0323
2R Co@PAT	356	145	321	67	3.30	16.3	577.1	0.0528
3R Co@PAT	329	119	300	74	4.29	14.4	509.9	0.0982
4R Co@PAT	**290**	**96**	**250**	**40**	**2.0**	**64.2**	**2273.3**	**0.1380**
5R Co@PAT	358	123	313	62	3.73	30.2	1069.4	0.0511

Table S3. Important another parameters of the present 4R Co@PAT catalyst.

Applications	Potential (V)	Tafel (mV/dec)	Durability (h)	R_{ct} (Ω)
Urea oxidation	**1.40**	**40**	**25**	**1.18**
Seawater splitting	**1.53**	**78.81**	**20**	**0.761**

Table S4: OER performance of 4R Co@PAT/GC in 1.0 M KOH was compared with previously reported nonprecious electrocatalysts.

S.NO	Catalyst/GC	η (mV) @ 10mA cm^{-2}	References
1.	**4R Co@PAT**	**290**	**This work.**
2.	Co nanoparticles	390	*J. Am. Chem. Soc.* 2015, 137, 7071–7074
3.	Ni^{2+}/birnessite	400	*Angew. Chem. Int. Ed.* 2016, 55, 10381–10385
4.	Cobalt-Phosphide Nanorods	320	*ACS Catal*. 2015, 5, 6874-6878
5.	Co_3O_4 nanoplates	523	*J. Mater. Chem. A.* 2015, 3, 8107-8114
6.	$CoCr_2O_4$	422	*Nat. Commun.* 2014, 5, 1-9
7.	Fe–CoOOH/G	330	*Adv. Energy Mater.* 2017, **7**, 1602148-1602157.
8.	NiCo cages	380	*Adv. Mater*. 2016, 28, 4601-4605
9.	Co_9S_8@MoS_2/CNF	430	*Adv. Mater*. 2015, 27, 4752-4759.
10.	CoCo-LDH 2D Nanomesh	319	*J. Mater. Chem. A*. 2019, **7**, 26905- 26910

Table S5: OER performance of 4R Co@PAT/NF in 1.0 M KOH was compared with previously reported nonprecious electrocatalysts.

S.NO	Catalyst/NF	η (mV) @ 10mA cm^{-2}	References
1.	**4R Co@PAT**	**250**	**This work**
2.	Crystalline CoP/NF	392	*J. Mater. Chem. A,* 2019. 7, 15749-15756.
3.	Co_3O_4/ $NiCo_2O_4$ DSNCs	340	*J. Am. Chem. Soc.* 2015, *137*, 5590-5595
4.	PANI-NiCo: before ADT	420	*Nano letters*.2015, 15, 1421-1427
5.	$NiCo_2O_4$ Octahedron	380	*J Catal*. 2018, *357*, 238-246
6.	CoP	290	*Adv. Funct. Mater*, 2015, 25, 7337-7347
10.	CoP-MNA	290	*Adv. Funct. Mater*, 2015, 25, 7337-7347
7.	Ni_3S_2 leaves	340	*J. Mater. Chem. A,*. 2016, 4, 13916-13922
8.	CoCo LDH	380	*Nat. Commun*. 2014, *5*, 4477
9.	Co_3O_4	339	*Angew. Chem*. 2016, 128, 8812-8816

Table S6: UOR performance of 4R Co@PAT/NF in 0.33 M Urea + 1.0 M KOH was compared with previously reported nonprecious electrocatalysts.

Catalysts	conc. of urea	Electrolyte	electrocatalytic activity	onset potential (vs RHE)	References
4R Co@PAT	**0.33 M**	**1.0 M KOH**	**10 mA cm^{-2}**	**1.29 V**	**This work**
La–Ni perovskite nanocluster-based composite	0.33 M	1.0 M KOH	14.7 mA cm^{-2}		*Synth. Met.* 2020, *266*, 116 372
NiCo/MWCN	1.0 M	1.0 M KOH	441.70 mA cm^{-2}		*Sci. Rep.* 2019, *9*, 479
Ni/Sn-dendrites	0.33 M	1.0 M KOH	44 mA cm^{-2}	1.34 V	*ChemElectroChem* 2017, *4*, 1037– 1043
Ag/ZnO	0.33 M	1.0 M KOH	12.0 mA cm^{-2}	1.41 V	*Electroanalysis* 201 9, *31*, 17– 21
rGO/LaNiO	0.33 M	1.0 M KOH	11.98 mA cm^{-2}		*. J. Electrochem. Soc.* 2018, *165*, J33 10
Ni–Fe double hydroxide	0.33 M	1.0 M NaOH	95 mA cm^{-2}		*New J. Chem.* 2017, *41*, 41 90– 4196
CoGC electrode	0.33 M	1.0 M KOH	6.4 mA cm^{-2}	1.31 V	*ACS omega*, 2020, *5*, 26038-26048

Table S7: Seawater performance of 4R Co@PAT/NF in 0.5 M NaCl + 1.0 M KOH was compared with previously reported nonprecious electrocatalysts

Catalysts	**Conc. of NaCl**	**η (mV) @ 10 mA cm^{-2}**	**References**
4R Co@PAT	**0.5 M**	**311**	**This work**
W2N/WC	-	320	*Adv. Mater*. 2020, 32 1905679.
PHI-Co	-	324	*Adv. Mater*. 2020, 32 1903942.
Co2Mo3O8@NC-800	-	331	*Angew. Chem. Int. Ed.* 2020, 59, 11948.
NCoM-SS-Ar	-	340	*Angew. Chem. Int. Ed.* 2019, 58, 8330.
NCoM-Cb-Ar		340	*Angew. Chem. Int. Ed.* 2019, 58, 8330.
COF-C4N		349	*ACS Energy Lett.* 2019, 4, 2251.
CoO/Co		350	*ACS Energy Lett.* 2017, 2, 1208.
Mo2C@N-CNTs		356	*Angew. Chem. Int. Ed.* 2019, 58, 4923.
Fe0.2Ni0.8@N-		380	Adv. Funct. Mater.

GR			2018, 28, 1706928.